Published in final edited form as:

Nature. 2016 November 17; 539(7629): 433–436. doi:10.1038/nature20128.

Transcription of the non-coding RNA upperhand controls *Hand2* expression and heart development

Kelly M. Anderson[1,2], **Douglas M. Anderson**[1,2], **John R. McAnally**[1,2], **John M. Shelton**[3], **Rhonda Bassel-Duby**[1,2], and **Eric N. Olson**[1,2]

[1]Department of Molecular Biology, University of Texas Southwestern Medical Center, Dallas, Texas 75390, USA

[2]Hamon Center for Regenerative Science and Medicine, University of Texas Southwestern Medical Center, Dallas, Texas 75390, USA

[3]Department of Internal Medicine, University of Texas Southwestern Medical Center, Dallas, Texas 75390, USA

Abstract

HAND2 is an ancestral regulator of heart development and one of four transcription factors that control the reprogramming of fibroblasts into cardiomyocytes[1–4]. Deletion of *Hand2* in mice results in right ventricle hypoplasia and embryonic lethality[1,5]. *Hand2* expression is tightly regulated by upstream enhancers[6,7] that reside within a super-enhancer delineated by histone H3 acetyl Lys27 (H3K27ac) modifications[8]. Here we show that transcription of a *Hand2*-associated long non-coding RNA, which we named upperhand (*Uph*), is required to maintain the super-enhancer signature and elongation of RNA polymerase II through the *Hand2* enhancer locus. Blockade of *Uph* transcription, but not knockdown of the mature transcript, abolished *Hand2* expression, causing right ventricular hypoplasia and embryonic lethality in mice. Given the substantial number of uncharacterized promoter-associated long non-coding RNAs encoded by the mammalian genome[9], the *Uph–Hand2* regulatory partnership offers a mechanism by which divergent non-coding transcription can establish a permissive chromatin environment.

In all well-annotated mammalian species, long non-coding RNA (lncRNA) transcripts with a similar intron–exon organization are transcribed upstream of the *Hand2* locus (Extended Data Fig. 1a, b). We refer to these transcripts as ‘upperhand’ (*Uph*), although the human transcripts have been referred to as *DEIN* (differentially expressed in neuroblastoma, also known as *HAND2-AS1*)[10]. Rapid amplification of cDNA ends (RACE) analysis of *Uph*

Correspondence and requests for materials should be addressed to E.N.O. (eric.olson@utsouthwestern.edu).

Online Content Methods, along with any additional Extended Data display items and Source Data, are available in the online version of the paper; references unique to these sections appear only in the online paper.

Author Contributions K.M.A., D.M.A. and E.N.O. designed experiments and analysed data. J.R.M. generated mutant mice from constructs designed and created by K.M.A. and D.M.A. K.M.A. performed qPCR, phenotypic analysis, dissections, ChIP, RNA immunoprecipitation, cardiomyocyte fractionation, Southern blot, and India ink injections. D.M.A performed northern blot, RACE, *in vitro* transcription/translation, and GapmeR transfections. J.M.S. and K.M.A. performed *in situ* hybridization and generated images. K.M.A., D.M.A, E.N.O. and R.B.D. wrote and edited the manuscript.

The authors declare no competing financial interests.

revealed several alternatively spliced transcripts in the mouse heart (Extended Data Fig. 1c). The major mouse *Uph* transcript is 770 nucleotides long, contains six exons, a polyadenylation sequence and shares a bidirectional promoter with *Hand2* (ref. 10; Fig. 1a). The mouse *Uph* locus encompasses ~16.5 kilobases and contains two enhancers that direct *Hand2* expression in the heart and branchial arches[6,7], as well as histone acetylation marks that delineate a cardiac super-enhancer in this locus[8] (Fig. 1a).

Similar to most characterized lncRNAs[11], the *Uph* nucleotide sequence is not well-conserved, with only ~56% homology between mouse and human, and little conservation across other species (Extended Data Fig. 1a). However, *Uph* orthologues share a promoter and contain the conserved *Hand2*-associated cardiac and brachial arch enhancers within their second introns (Extended Data Fig. 1b).

Promoter-associated lncRNAs are often positively correlated with transcription of their protein-coding neighbour[12,13]. Indeed, whole-mount *in situ* hybridization for *Uph* in mouse embryos revealed expression in the heart, distal branchial arches and the developing limb bud at embryonic day (E)10.5, overlapping with *Hand2* expression (Extended Data Fig. 1d). *Uph* expression was strong in the heart and continued to mirror *Hand2* at later fetal stages (Fig. 1b). Northern blot analysis across several adult tissues revealed that *Uph* transcript levels were highest in the heart (Extended Data Fig. 1e).

Cell fractionation of mouse neonatal cardiomyocytes showed *Uph* transcripts in all fractions but enrichment in the cytoplasm, similar to 18S RNA (Extended Data Fig. 2a). The distribution of *Uph* differed from nuclear lncRNAs such as *Malat1*, which associates with chromatin (Extended Data Fig. 2a). Previously, we reported that some annotated lncRNAs can encode micropeptides[14,15]. However, *Uph* does not contain a conserved open reading frame and *in vitro* transcription and translation of *Uph* did not produce any detectable peptides (Extended Data Fig. 2b). Together, these data reveal that *Uph* is a bona fide lncRNA that is co-expressed in a temporal and tissue-specific pattern with the essential cardiac transcription factor *Hand2*.

To examine *Uph* function *in vivo*, we used transcription activator-like effector nucleases (TALENs) to insert a triple polyadenylation sequence into exon 2 of the *Uph* locus in C57BL/6 mouse zygotes (Extended Data Fig. 3a). To avoid potential regulatory elements required for *Hand2* expression, we inserted the triple polyadenylation cassette into a region with low sequence conservation. Furthermore, we generated a separate knock-in allele using a heterologous DNA sequence (tdTomato (tdTO) lacking a polyadenylation sequence) inserted into the same *Uph* locus (Extended Data Fig. 3b). Correct targeting of the triple polyadenylation and tdTO sequences was verified by Southern blot analysis (Extended Data Fig. 3c, d).

Mice homozygous for the *Uph* tdTO allele ($Uph^{tdTO/tdTO}$) were born at expected Mendelian ratios and showed no morphological defects or notable changes in *Uph* or *Hand2* expression (Extended Data Fig. 3e, f). Thus, insertion of a heterologous DNA sequence into exon 2 of the *Uph* locus is not sufficient to disrupt normal *Hand2* expression. However, from 31 pups

born of heterozygous *Uph* (*Uph*$^{+/-}$) intercrosses, no *Uph*-knockout (KO) offspring survived, suggesting that *Uph* transcription is required for embryonic survival.

To pinpoint the embryonic death of *Uph* KO embryos, we collected embryos from timed pregnancies of *Uph*$^{+/-}$ matings. *Uph* KO embryos in a pure C57BL/6 background were present at approximate Mendelian ratios before E9.5 (20.6%; 13 out of 63 embryos collected), and showed no obvious size or morphological differences relative to wild-type littermates. However, by E10.5, the *Uph* KO embryos had a large pericardial effusion surrounding the heart and were growth restricted (Fig. 2a). Quantitative real-time PCR (qPCR) showed that *Uph* transcripts were reduced by 97% in *Uph* KO compared to wild-type hearts at E10.5, confirming successful termination of *Uph* transcription (Extended Data Fig. 3g). Histological analyses revealed that hearts from *Uph* KO embryos failed to develop a right ventricular chamber. Instead, the outflow tract and atrial chamber connected to a single left-sided ventricular chamber (Fig. 2b), a cardiac phenotype reminiscent of *Hand2* KO embryos.

Because *Uph* KO embryos displayed a similar cardiac phenotype to *Hand2* KO embryos, we analysed the expression of *Hand2* and other cardiac transcription factors in *Uph* KO embryos using *in situ* hybridization. Notably, *Hand2* expression was absent in the atria, ventricle and outflow tract of *Uph* KO embryos, but remained detectable, albeit at reduced levels, in the branchial arches and limb buds (Fig. 3a, Extended Data Fig. 4a). Consistent with the persistent expression of *Hand2* in the branchial arches, *Uph* KO embryos lacked the vascular defects in the aortic arch arteries and the aortic sac typically seen in *Hand2* mutant embryos[1,5] (Extended Data Fig. 4b). Genes encoding other cardiac transcription factors essential for cardiac morphogenesis, namely *Nkx2-5*, *Gata4* and the related *Hand1*, were not considerably changed in *Uph* KO embryos (Fig. 3b, Extended Data Fig. 4a), demonstrating the specificity of *Uph* transcription in regulating *Hand2* expression.

To determine whether *Uph* functions in *cis* or *trans* to regulate *Hand2*, we intercrossed mice carrying a *Hand2* KO allele with mice carrying the *Uph* KO allele, to generate compound heterozygous (*Uph*$^{+/-}$ *Hand2*$^{+/-}$) embryos. Notably, *Uph*$^{+/-}$ *Hand2*$^{+/-}$ embryos recapitulated the *Uph* KO phenotype, displaying pericardial effusion and embryonic lethality by E10.5 (Fig. 4a, Extended Data Fig. 5a). While *Uph* expression was not reduced in compound heterozygotes, *Hand2* expression was decreased by greater than 90% (Extended Data Fig. 5b). These findings demonstrate that expression of *Hand2* in the heart is dependent on transcription of *Uph* in *cis*, which cannot be compensated for by *Uph* transcripts generated on the sister allele.

Several lncRNAs have been proposed to function by recruiting the trithorax chromatin-modifying complex to gene loci[16,17]. To determine whether *Uph* interacts with the trithorax complex, we performed RNA immunoprecipitation using an antibody against the RNA-binding adaptor of the MLL-1 trithorax protein, WDR5. While the lncRNA HOTTIP formed a stable complex with WDR5 in the mouse HL-1 cardiomyocyte-like cell line[18], we could not detect an interaction between MLL-1 and *Uph* (Extended Data Fig. 5c).

To determine whether the mature *Uph* RNA transcript is required for *Hand2* expression, we performed knockdown of *Uph* using GapmeR antisense oligonucleotides[19] in HL-1 cells and in the neuroblastoma cell line Neuro2a, both of which express *Uph* and *Hand2* (Extended Data Fig. 6a). Knockdown of mature *Uph* transcripts by more than 90% using two different GapmeR oligonucleotides in both cell lines did not alter *Hand2* expression (Extended Data Fig. 6b, c). Because *Uph* is alternatively spliced, we performed qPCR across all *Uph* exon junctions (Extended Data Fig. 6d). We further verified that efficient knockdown was attained in the nuclear fraction of HL-1 cells (Extended Data Fig. 6e). Additionally, overexpression of the full-length *Uph* transcript in HL-1 cells using transient transfection had no effect on the levels of *Hand2* mRNA (Extended Data Fig. 6f). Together, these data suggest that, in contrast to premature transcriptional termination of *Uph in vivo*, the mature *Uph* transcript is not required for *Hand2* expression.

DNA loci with high regulatory capacity such as enhancers[20,21], polycomb response elements[22,23] or locus control regions[24] are often associated with non-coding transcription and can function to maintain a permissive histone signature. In the developing heart, the super-enhancer at the *Hand2* locus is defined by H3K27ac (Fig. 4b). To test whether *Uph* transcription is required to maintain the enhancer signature in the *Uph–Hand2* locus, we performed chromatin immunoprecipitation (ChIP) on *Uph* KO and wild-type E10.0 hearts, using H3K4me1 and H3K27ac active enhancer marker antibodies. We found that the H3K4me1 and H3K27ac peaks normally established at the *Uph–Hand2* locus were reduced in *Uph* KO hearts (Fig. 4c, d).

The GATA4 transcription factor is required for activation of the HAND2 cardiac enhancer in the *Uph* locus, and participates in establishing active H3K27ac marks[7,25]. We observed a reduction in GATA4 binding to the *Hand2* cardiac enhancer in *Uph* KO hearts, a finding consistent with the reduced H3K27ac enhancer marks in the *Uph* locus (Fig. 4e). We observed no differences in H3K4me1 or H3K27ac levels at an active enhancer in the promoter region of *Nkx2-5*, no differences in GATA4 binding to the *Nkx2-5* promoter, and no differences in H3K27me3 repressive marks between wild-type and *Uph* KO embryos at the *Uph–Hand2* locus (Extended Data Fig. 7b–f).

Enhancer-associated histone acetylation is necessary for gene expression by promoting RNA polymerase II (RNAPII) elongation at gene promoters[26]. To measure the levels of RNAPII at the *Hand2* locus, we performed ChIP on wild-type and *Uph* KO E10.0 hearts using the Ser2-phosphorylated RNAPII antibody, a marker of RNAPII elongation, at the *Hand2* locus. Although there was no difference in RNAPII recruitment to the *Hand2* transcriptional start site, RNAPII binding to the body of the *Hand2* locus was decreased in *Uph* KO hearts (Fig. 4f). We found no differences in Ser2-phosphorylated RNAPII binding to the *Nkx2-5* gene body between genotypes (Extended Data Fig. 7g). These findings suggest that the loss of GATA4 and histone acetylation marks in the *Uph–Hand2* locus of *Uph* KO hearts prevents RNAPII elongation within the *Hand2* locus.

Here we define the *in vivo* function of *Uph*, a cardiac-enriched lncRNA co-transcribed bi-directionally with the cardiac transcription factor *Hand2.* Termination of *Uph* transcription, but not of the mature transcript, resulted in the loss of *Hand2* expression in the heart and

partially phenocopied the lethal cardiac defects observed in *Hand2* KO embryos. Compound $Uph^{+/-}$ $Hand2^{+/-}$ heterozygosity causes embryonic lethality, suggesting that transcription of *Uph* is required in *cis* to promote *Hand2* expression. Termination of *Uph* transcription *in vivo* reduced GATA4 binding and the *Uph–Hand2* super-enhancer signature, resulting in RNAPII pausing and loss of *Hand2* expression in the heart. We predict that transcription of *Uph* governs *Hand2* expression in all tissues for which the expression of *Hand2* depends on enhancers located within the *Uph* locus. Future studies are needed to determine the role of *Uph* in the regulation of *Hand2* in non-cardiac tissues, which are currently precluded owing to early embryonic lethality of the global *Uph* KO. Given the importance of *Hand2* in the development of the palate, tongue, limbs, and sympathetic nervous system[27–30], *Uph* provides a potentially important non-coding regulatory mechanism for the temporal and spatial control of *Hand2* expression.

METHODS

Animal models

All experimental procedures involving animals in this study were reviewed and approved by the University of Texas Southwestern Medical Center's Institutional Animal Care and Use Committee. Animals/embryos were allocated to experimental groups based on genotype and we did not use exclusion, randomization or blinding approaches. The sex of embryos used in these studies was not determined. In general, sample size was chosen to use the least number of animals/embryos to achieve statistical significance and no statistical methods were used to predetermine sample size.

In situ hybridization

Whole mount *in situ* hybridization was performed using digoxigenin-labelled antisense RNA probes specific to *Uph* and *Hand2*, using methods previously described[31]. Radioisotopic *in situ* hybridization studies on sections were performed as previously described[32]. Antisense RNA probe templates for *Uph* or *Hand2* were generated using mouse heart cDNA and subcloned into pCRII TOPO (Life Technologies). Primer sequences are listed in Extended Data Table 1.

Subcellular fractionation of mouse neonatal cardiomyocytes

Neonatal cardiomyocytes were collected from ~50 post-natal day 1 (P1) C57BL/6 mice using the Neomyt kit (Cellutron, nc-6031) and fractionated as previously described[33].

TALEN-mediated homologous recombination in mice

A TALEN pair specific for the *Uph* locus was designed using the ZiFiT Targeter Program (http://zifit.partners. org/ZiFiT/Introduction.aspx). Individual TALEN modules and donor vectors were constructed and assembled as previously described[14]. TALEN mRNAs and circular DNA donor plasmids were diluted to 25 ng μl^{-1} and 3 ng μl^{-1}, respectively, and co-injected into the nucleus and cytoplasm of one-cell stage C57BL/6 zygotes and transferred into pseudopregnant mice. Cloning and genotyping primer sequences are listed in Extended Data Table 1.

Histology

Embryos were fixed in 4% formaldehyde in PBS and processed for paraffin histology, sectioned and stained with haematoxylin and eosin using routine procedures. At least 5 embryos of each genotype were sectioned for all experiments and data reported are representative of all samples collected.

ChIP

ChIP was performed using the SimpleChIP Kit (Cell Signaling, 9004) with the following adjustments to the standard protocol. In brief, embryonic hearts were dissected from E10.0 embryos and flash frozen in liquid nitrogen. On average, 5 hearts from identical genotypes were pooled in a 1.5 ml tube before formaldehyde cross-linking. Sonication was performed using a Bioruptor (Diagenode). The following antibodies were used: 10 μl H3K4me1 (Abcam, ab8895), 10 μl histone H3 (Cell Signaling), 10 μl H3K27ac (Active Motif, 39133), 10 μl H3K27me3 (Active Motif, 39155), 5 μl RNA polymerase II CTD repeat YSPTSPS (phospho S2) (Abcam, ab5095), 5 μl of GATA4 (sc-1237X). qPCR primer sequences are listed in Extended Data Table 1.

GapmeR antisense oligonucleotide knockdown of *Uph* in HL-1 and Neuro2a cells

The mouse neuroblastoma cell line Neuro2a was purchased from ATCC and authenticated by morphology. The cardiomyocyte-like cell line HL-1 was donated by the laboratory of W. Claycomb. Contamination from mycoplasma was not tested for in these cell lines. LNA longRNA GapmeR oligonucleotides specific for *Uph* were designed and purchased from Exiqon. HL-1 and Neuro2a cells were co-transfected with a plasmid encoding eGFP (CS2GFP, 0.3 ng μl^{-1} final) and 50 nM GapmeR antisense oligonucleotides using Lipofectamine2000 (Life Technologies), according to the manufacturer's recommended protocol. Two days after transfection, GFP-positive cells were FACS sorted and processed using TRIzol (Life Technologies) for downstream gene expression analyses. GapmeR antisense oligonucleotide sequences are listed in Extended Data Table 1.

RACE PCR

The sequences of *Uph* RNA transcripts expressed in the mouse heart were determined using 5′ and 3′ RACE PCR using commercially available Marathon-Ready cDNA (Clontech). RACE PCR was performed according to manufacturer's recommended protocol, using primers specific to exon 4 of *Uph* and the marathon adaptor primer 1 (AP1). 5′ and 3′ *Uph* primer sequences are listed in Extended Data Table 1.

RNA immunoprecipitation

RNA–protein complexes from formaldehydecross-linked HL-1 cell lysates were immunoprecipitated using 2 μl IgG (Cell Signaling) or 2 μl WDR5 (Cell Signaling) antibodies. RNA purification and expression analyses were performed as previously described[34].

Statistics

Unless otherwise indicated in the figure legends, error bars represent s.e.m. of at least 3 biological replicates of each genotype or sample.

Data availability

Expressed sequence tag (EST) sequences for alignment of *Uph* transcripts were downloaded from GenBank: rat (BF567084), pig (DN117952), dog (DN434464) and cow (DN282558), or from RefSeq: human (NR_003679.2). Previously published ChIP–seq data used in Fig. 4b and Extended Data Fig. 7a, b are available under accession code GSE31039 (ref. 35). Source data for Extended Data Figs 1e, 2b, 3c, d are available in Supplementary Fig. 1, and all other data that support the findings of this study are available from the corresponding author on request.

Extended Data

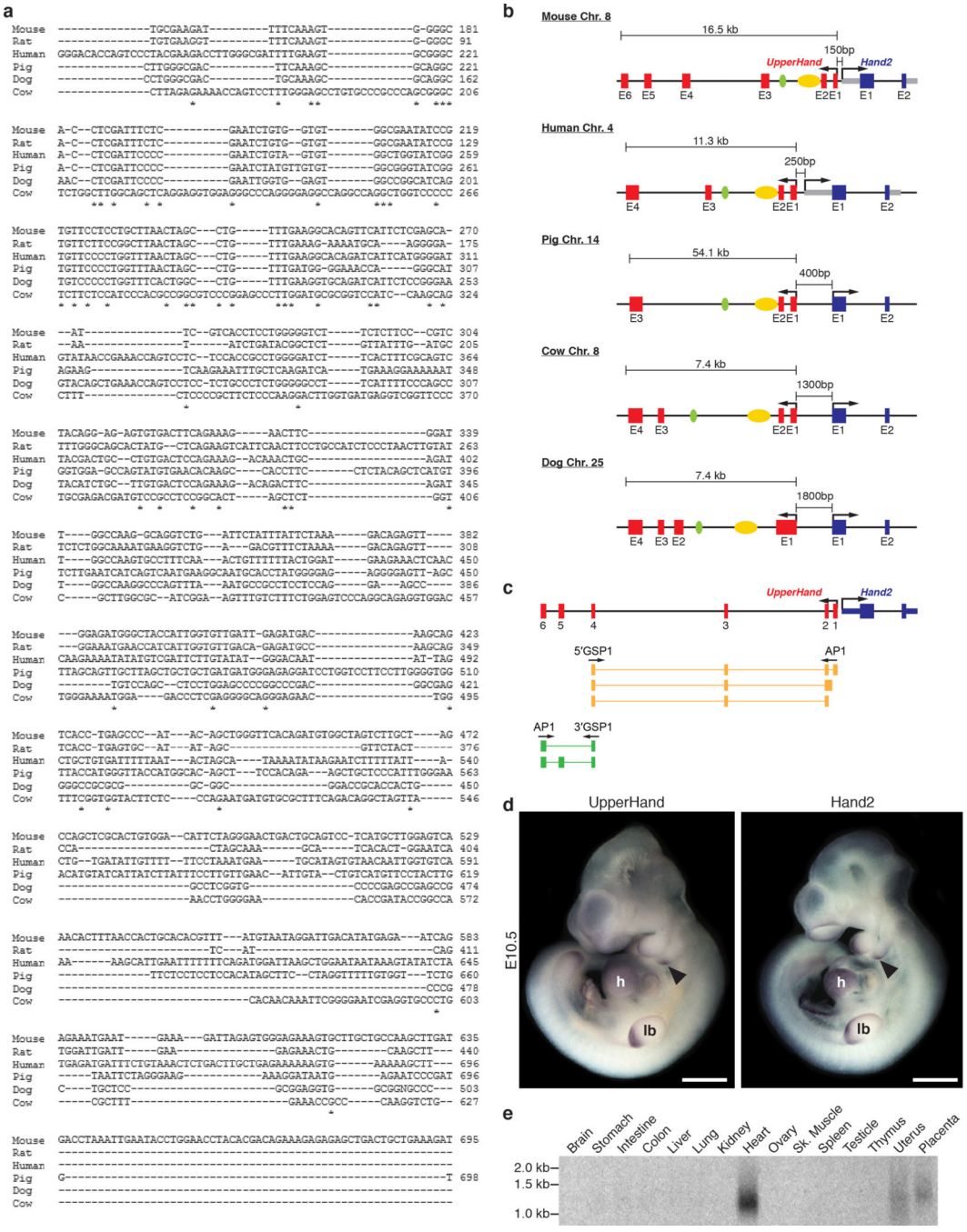

Extended Data Figure 1. Sequence alignment of several mammalian *Uph* transcripts

a, Sequence alignment of several mammalian *Uph* transcripts performed using ClustalW. See Methods for source data. **b**, Diagram of the *Hand2* locus in mammals showing the genomic organization and orientation of *Uph*. The *Hand2* branchial arch enhancer (green) and cardiac enhancer (yellow) are shown. **c**, Diagram of the *Uph* transcripts expressed in the mouse heart, determined using 5′ and 3′ RACE using primers specific to exon 4 of *Uph*.

AP1, marathon adaptor primer; 3′ GSP, 3′ *Uph*-specific primer from exon 4; 5′ GSP, 5′ *Uph*-specific primer from exon 4. **d**, Whole mount *in situ* hybridization of E10.5 mouse embryos. Expression was detected in heart, branchial arches (arrowhead), and limb bud. Scale bars, 1 mm. **e**, Northern blot analysis of total RNA from adult mouse tissues using a probe specific to the major *Uph* transcript. For gel source data, see Supplementary Fig. 1.

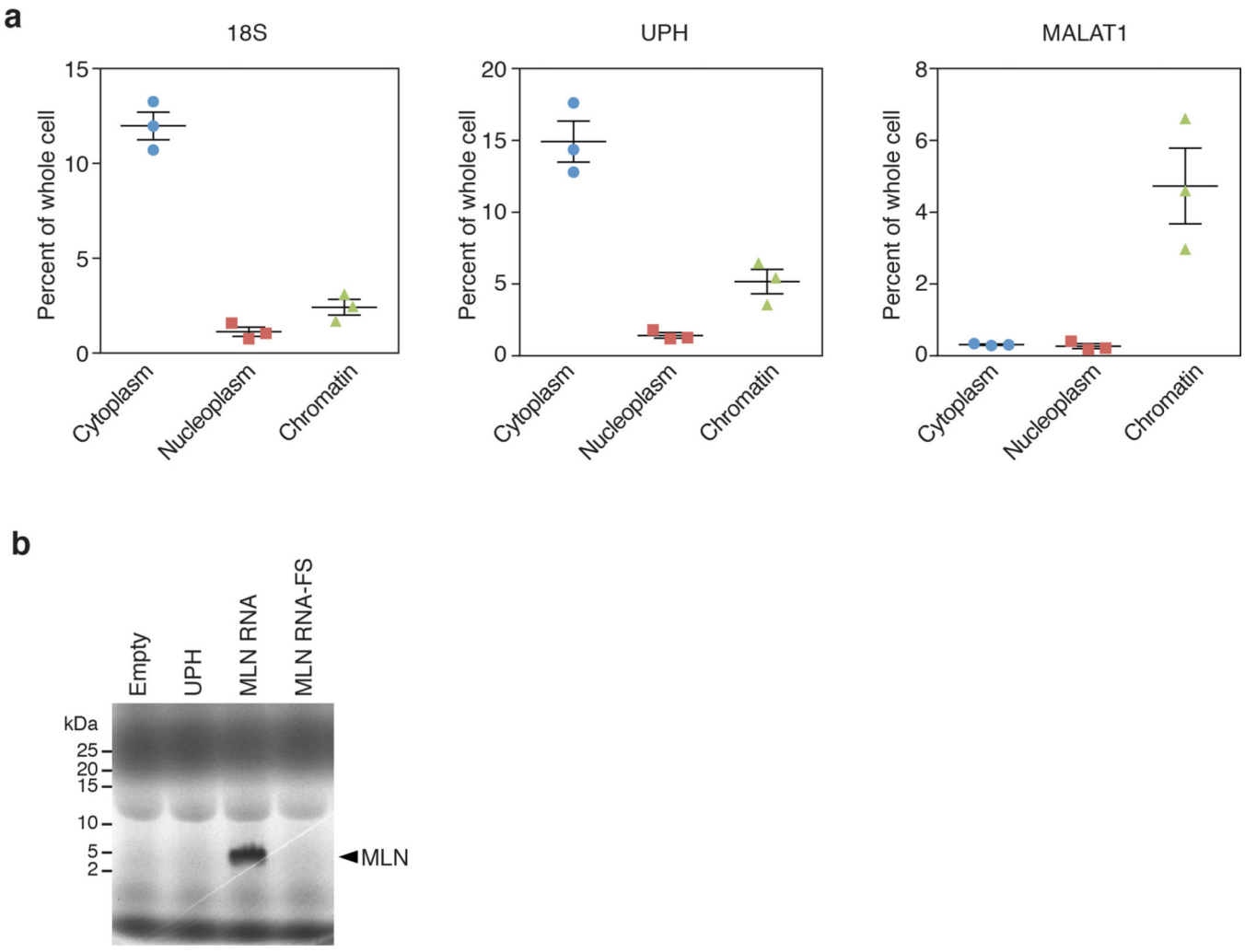

Extended Data Figure 2. *Uph* is a cytoplasmic lncRNA

a, Subcellular fractionation of 18S, *Uph* and *Malat1* lncRNA in mouse neonatal cardiomyocytes ($n = 3$ biological replicates from 1 of 5 independent experiments; mean ± s.e.m.). **b**, *In vitro* transcription and translation of a plasmid encoding the major *Uph* RNA. A plasmid encoding the myoregulin (MLN) micropeptide was used as a positive control, and myoregulin with a frameshift mutation (MLN RNA-FS) was used as a negative control. In contrast to myoregulin, *Uph* and the negative control (MLN RNA-FS) did not produce any detectable proteins, indicating that *Uph* is a bona fide lncRNA. For gel source data, see Supplementary Fig. 1.

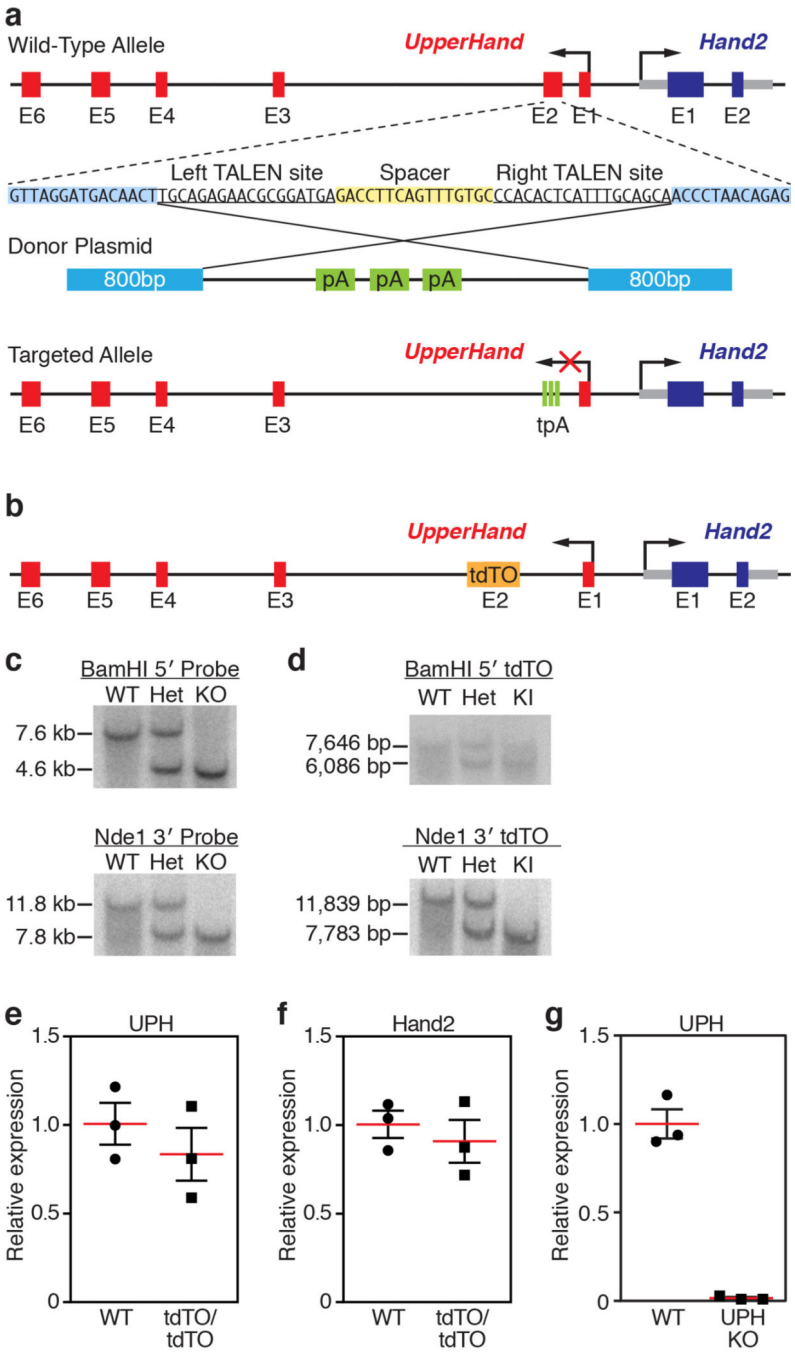

Extended Data Figure 3. Targeting strategy for insertion of transcriptional termination or heterologous sequence into exon 2 of *Uph*

a, *Uph* KO targeting strategy. Transcription activator-like effector nucleases (TALENs) were used to insert a triple polyadenylation (tpA) termination sequence into exon 2 (E2) of *Uph*. **b**, Using the same TALEN pair as in **a**, we introduced the coding sequence of tdTO, lacking a polyadenylation sequence, into exon 2 of the *Uph* locus. Exon 2, which includes the tdTO coding sequence, was spliced out of the mature *Uph* transcript, preventing expression of tdTO in these mice. **c**, Southern blot analysis of wild-type, heterozygous $Uph^{+/-}$ (Het) and

Uph KO genomic DNA. BamHI-digested DNA hybridized with a 5′ -specific probe and NdeI-digested DNA hybridized with a 3′ -specific probe. For gel source data, see Supplementary Fig. 1. **d**, Southern blot analysis of wild-type, $Uph^{tdTO/+}$ heterozygous and $Uph^{tdTO/tdTO}$ knock-in (KI) genomic DNA verified the correct targeting of the tdTO sequence into the *Uph* locus. DNA was digested with BamHI and hybridized with a 5′ -specific probe or digested with NdeI and hybridized with a 3′ -specific probe. For gel source data, see Supplementary Fig. 1. **e, f**, Expression of *Uph* (**e**) and *Hand2* (**f**) in wild-type and $Uph^{tdTO/tdTO}$ homozygous mice at E10.0 was not changed by the insertion of the tdTO sequence into exon 2 of the *Uph* locus ($n = 3$, representative of 3 independent experiments; mean ± s.e.m.). **g**, qPCR shows *Uph* transcripts decreased by ~97% in E10.5 hearts ($n = 3$ mice of each genotype from 1 of 3 independent experiments; mean ± s.e.m.).

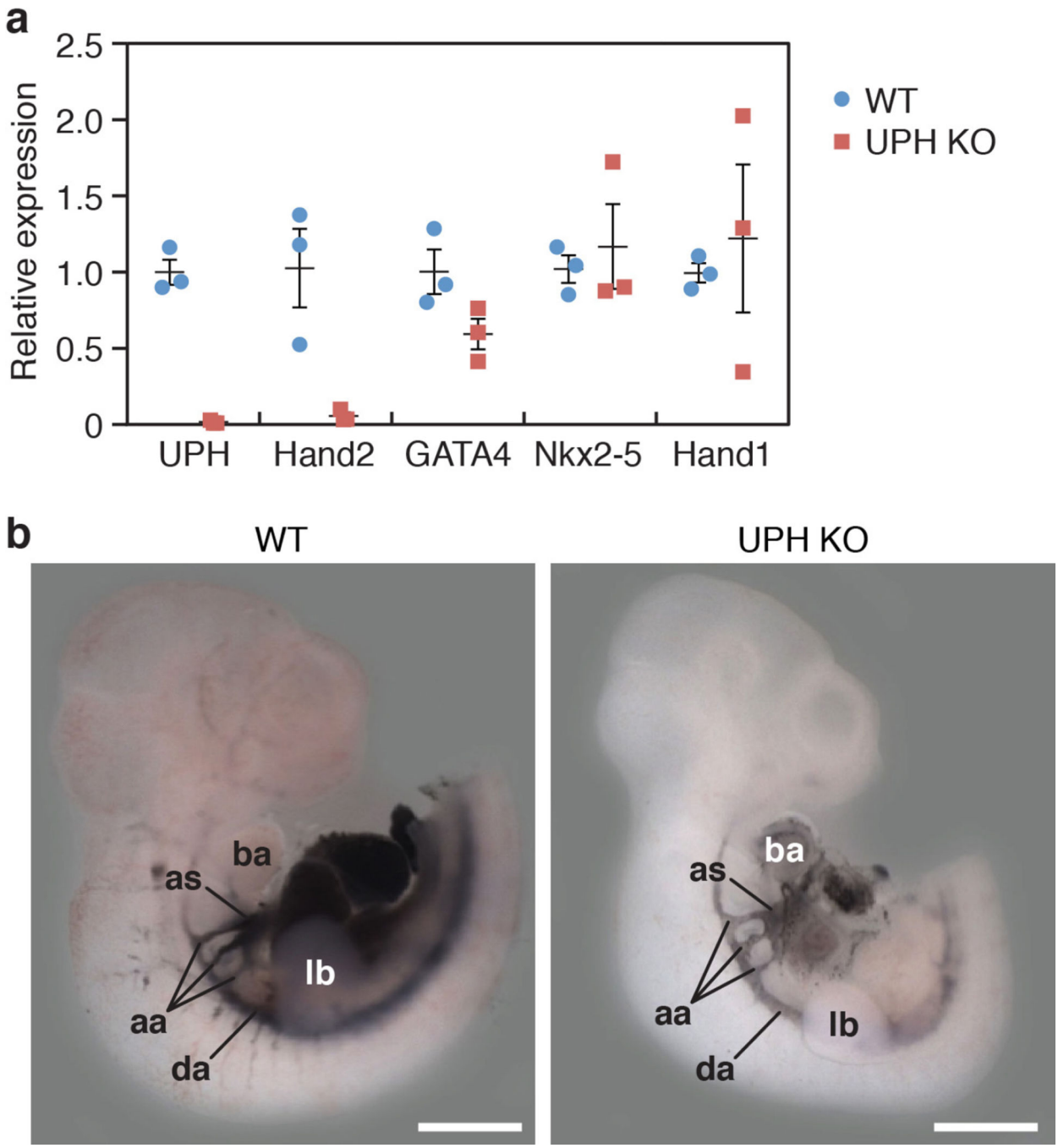

Extended Data Figure 4. Aortic arch arteries are normal in *Uph* KO embryos

a, qPCR quantification of gene expression at E10.0 showed robust downregulation of *Uph* and *Hand2* expression in *Uph* KO hearts, with normal expression of other cardiac transcription factors (n = 3 mice of each genotype from 1 of 3 independent experiments; mean ± s.e.m.). **b**, India ink was injected into either the left ventricle of wild-type embryos or the single ventricle of *Uph* KO embryos at E10.5, to visualize the aortic arch arteries and circulation, which appeared normal in *Uph* KO embryos. aa, aortic arch arteries; as, aortic sac; da, dorsal aorta. Scale bars, 1 mm.

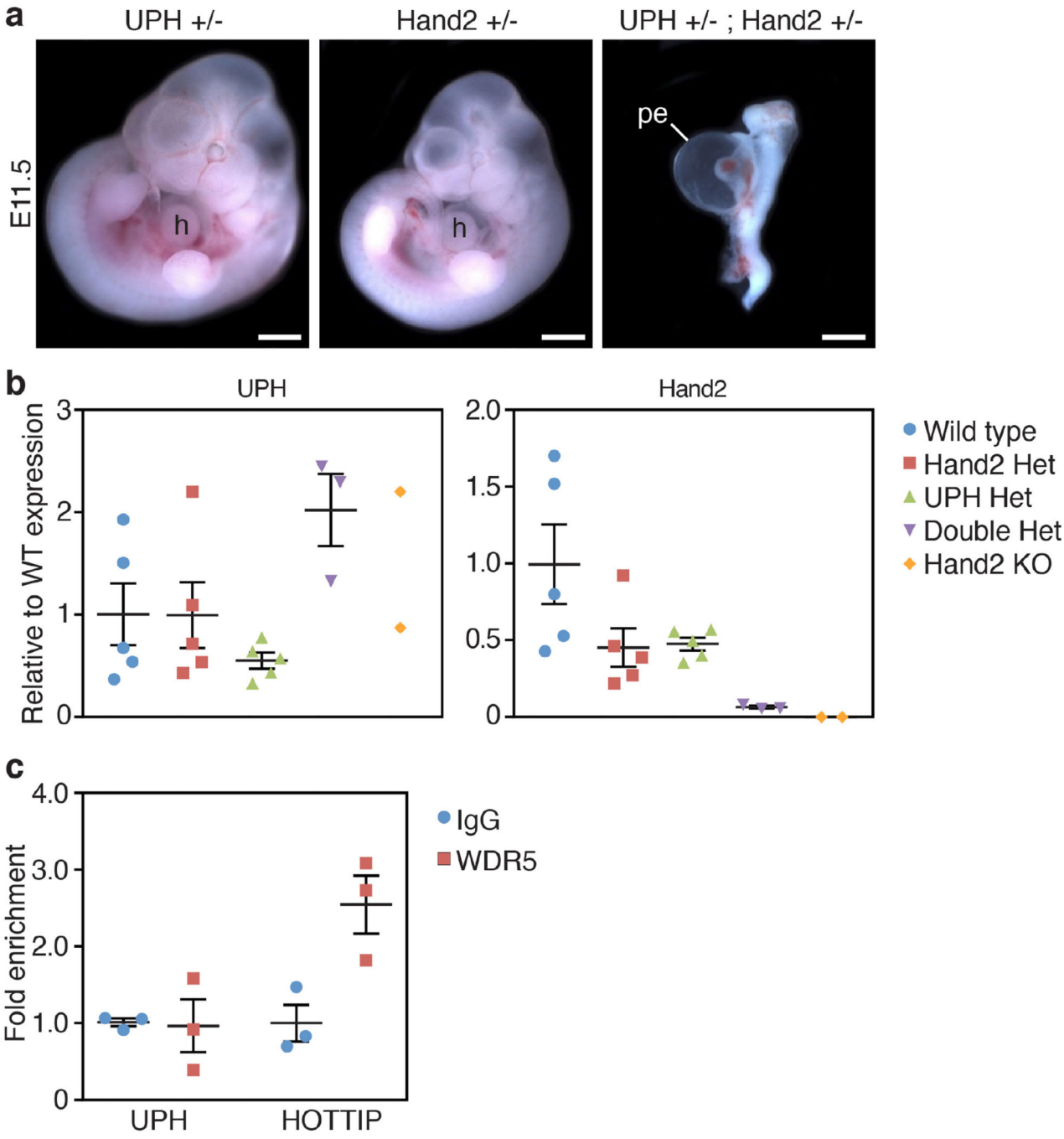

Extended Data Figure 5. *Uph*$^{+/-}$ *Hand2*$^{+/-}$ compound heterozygotes recapitulate *Uph* KO phenotype

a, *Uph*$^{+/-}$ *Hand2*$^{+/-}$ double heterozygote embryos developed a single ventricle, pericardial effusion, and were severely growth restricted by E11.5. Scale bars, 1 mm. **b**, *Uph* expression is normal in double heterozygotes, whereas *Hand2* was reduced by ~90%, relative to wild-type embryos (n = 5 mice for wild type, *Hand2* het and *Uph* het, n = 3 for double het, n = 2 for *Hand2* KO, from 1 of 2 independent experiments; mean ± s.e.m.). **c**, Immunoprecipitation of RNA using either IgG or WDR5 in HL-1 cells followed by qPCR

for *Uph* revealed no binding to WDR5. The WDR5-interacting lncRNA HOTTIP was used as a positive control (n = 3 biological replicates from 1 of 3 independent experiments; mean ± s.e.m.).

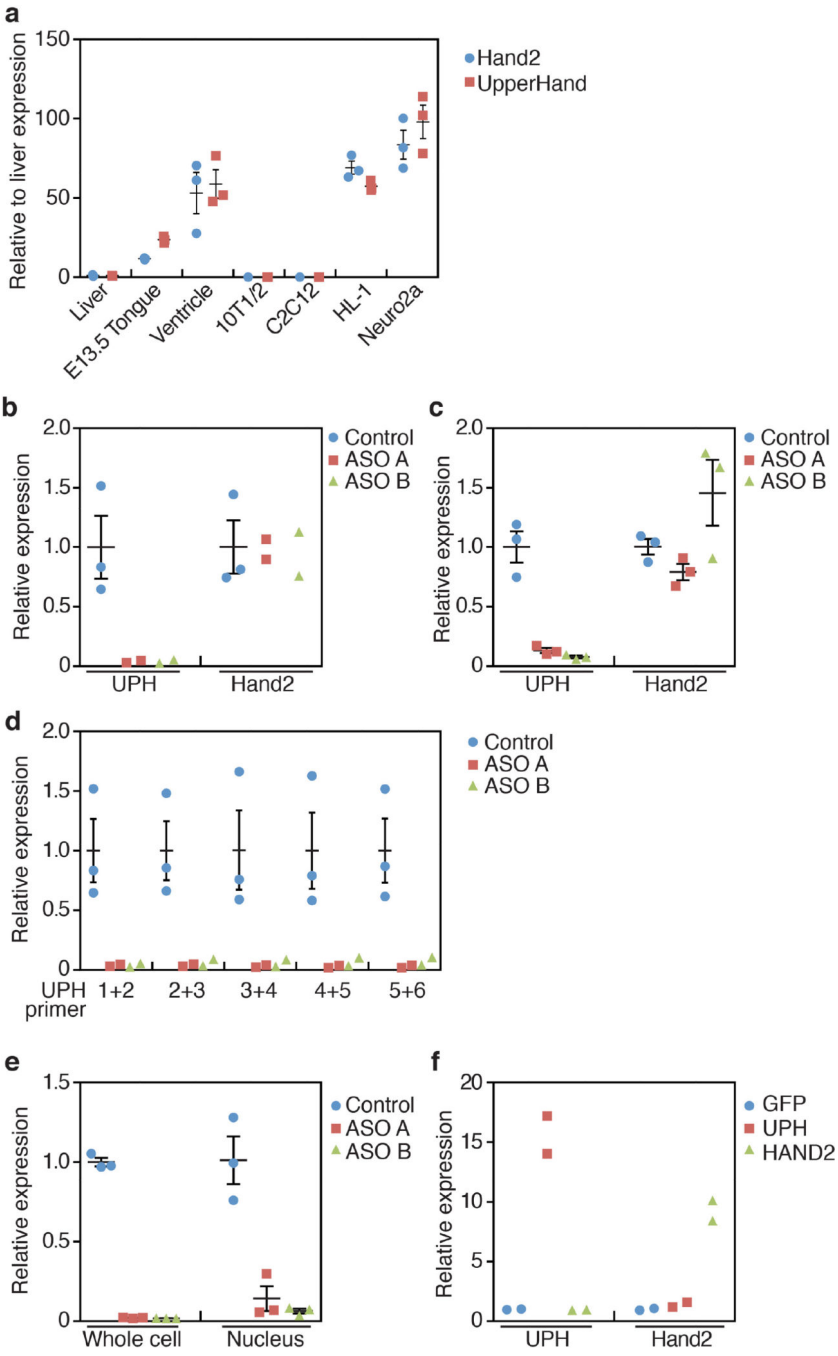

Extended Data Figure 6. Knockdown of mature *Uph* transcripts in HL-1 or Neuro2a cells does not affect *Hand2* expression

a, Expression of *Uph* (red) and *Hand2* (blue) in various tissues and cell lines. *Uph* and *Hand2* are robustly expressed in the heart, and the HL-1 and Neuro2a cell lines. *Uph* and *Hand2* transcripts are not expressed in the liver, 10T1/2 fibroblasts or skeletal muscle C2C12

myotubes (n = 3 technical replicates; mean ± s.e.m.). **b, c**, *Uph* transcripts were reduced by ~90% in HL-1 (**b**) and Neuro2a (**c**) cells when transfected with two independent GapmeR antisense oligonucleotide probes (ASO A and B) against *Uph*. Expression of *Hand2* was not changed (n = 2 for ASO A and B, n = 3 for control, from 1 of 2 independent experiments; mean ± s.e.m.). **d**, *Uph* transcripts were similarly downregulated across each exon–exon junction, measured using qPCR (n = 2 for ASO A and B, n = 3 for control, from 1 of 2 independent experiments; mean ± s.e.m.). **e**, Fractionation of HL-1 cells transfected with control or *Uph*-specific ASOs. The nuclear fraction of antisenseoligonucleotide-treated HL-1 cells showed a similar downregulation of *Uph* transcripts (n = 3 biological replicates from 1 of 3 independent experiments; mean ± s.e.m.). **f**, Overexpression of enhanced green fluorescent protein (eGFP; blue), the major *Uph* RNA (red) or *Hand2* RNA (green) in HL-1 cells revealed that the mature *Uph* transcript did not alter *Hand2* expression relative to wild type, and that *Hand2* does not influence the expression of *Uph* in these cells (n = 2 biological replicates from 1 of 2 independent experiments; mean ± s.e.m.).

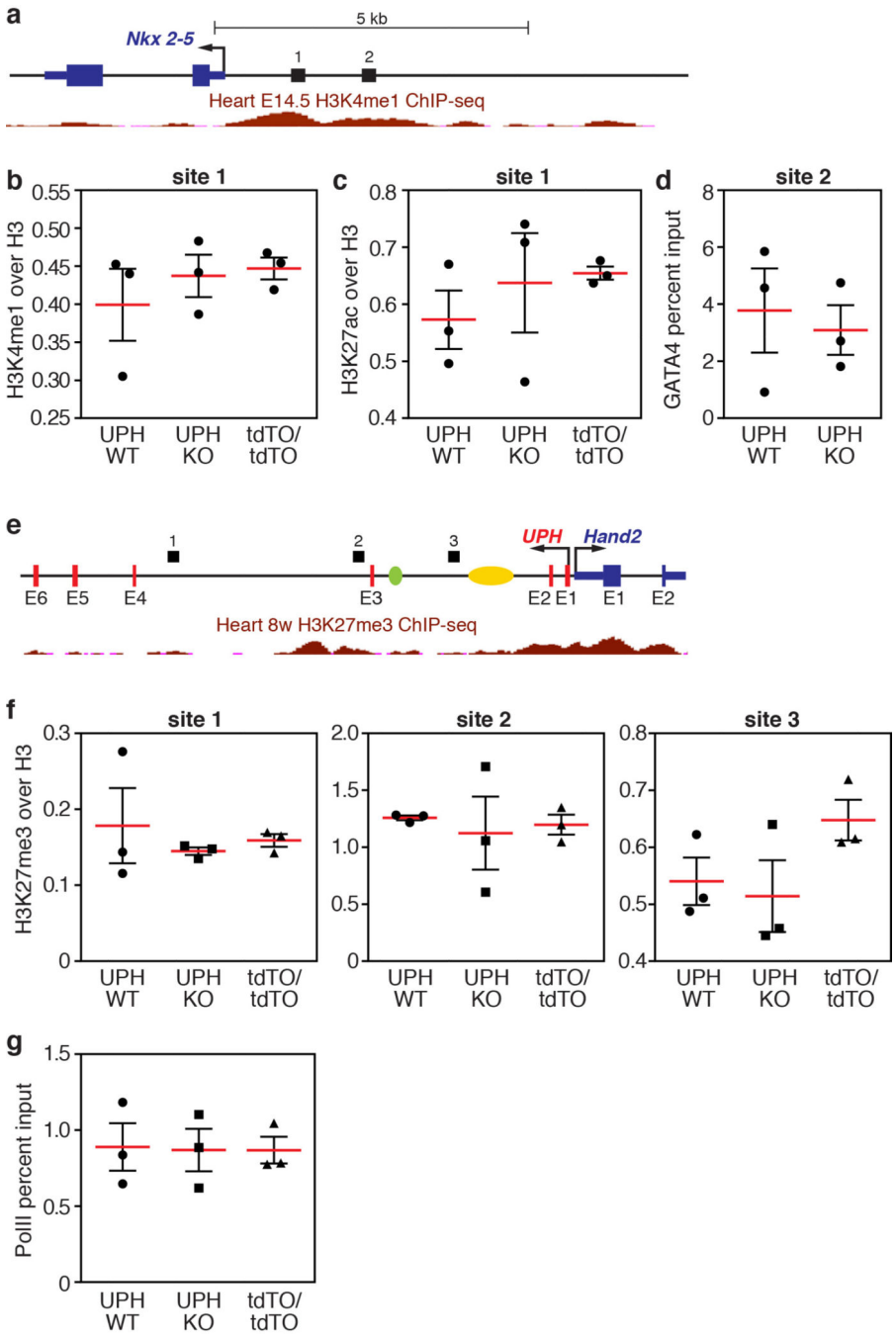

Extended Data Figure 7. ChIP and qPCR analyses of active cardiac enhancers regulating *Nkx2-5* expression

a, Diagram of the *Nkx2-5* locus with numbers (1 and 2) indicating the region analysed by qPCR following ChIP. Shown in red are the ENCODE/LICR H3K4me1 active enhancer marks in the heart at E14.5. See Methods for source data. **b**, ChIP coupled with qPCR analysis of H3K4me1 marks, normalized to total histone H3, showed that the H3K4me1 marks bound to the *Nkx2-5* promoter region are unchanged between wild-type, *Uph* KO and *Uph*$^{tdTO/tdTO}$ homozygous hearts at E10.0. **c**, ChIP coupled with qPCR analysis of H3K27ac

marks, normalized to total histone H3, showed that the H3K27ac marks bound to the *Nkx2-5* promoter region are unchanged between wild-type, *Uph* KO and $Uph^{tdTO/tdTO}$ homozygous hearts at E10.0. **d**, GATA4 binding to a GATA4 site in the *Nkx2-5* promoter is unchanged between wild-type and *Uph* KO hearts at E10.0. **e**, Diagram of the *Uph–Hand2* locus, with black bars indicating the regions analysed by qPCR following ChIP. Shown in red is the ENCODE/LICR H3K27me3 track for mouse heart. See Methods for source data. The branchial arch enhancer (green) and cardiac enhancer (yellow) are shown. **f**, ChIP coupled with qPCR analysis of the polycomb repressive marker H3K27me3, normalized to total histone H3, showed no differences between genotypes at each locus (1–3) indicated in the diagram in **e. g**, qPCR revealed no difference in the levels of Ser2-phosphorylated RNAPII between genotypes at the *Nkx2-5* gene body. Each point is one of 3 technical replicates of 5 pooled hearts for each genotype in each ChIP experiment, from 1 of 2 independent experiments; mean ± s.e.m.

Extended Data Table 1

Relevant sequences

SEQUENCE NAME	FORWARD	REVERSE
Full Length UPH sequence	CACTCATAACCATAAGATAATTAAAACGG	TTTAAAAAATAATTTTTAATATACTATGTGCATGGTTGGATAGGT
UPH qPCR primers	CATTCTCGAGCAATTCGTCA	TGGTAGCCCATCTCCAACTC
UPH ISH probe	GATGAGACCTTCAGTTTGTGCC	ATACTATGTGCATGGTTGGATAGGT
Hand2 ISH probe	ATGAGTCTGGTGGGGGGC	TCACTGCTTGAGCTCCAGG
UPH targeting 5 ' arm	TATCGGAGCTCGCACCTCGGAGCTGGGAA	GATACGCGGCCGCGGATCCAGTTGTCATCCTAACTTGGGTCA
UPH targeting 3 ' arm	TATCGGCTAGCCATATGACCCTAACAGAGATTGCGAAGA	GATACATCGATCAGGGCAGTTAGGTCTCAGC
UPH 5 ' WT genotyping	CTCCTCTCCGGACAAGAATC	TGCTGCAAATGAGTGTGG
UPH 5 ' KO genotyping	CTCCTCTCCGGACAAGAATC	GGTTCCGGATCCACTAGTTCT
UPH 3 ' WT genotyping	AGAGAACGCGGATGAGACCT	CCCTTGCAAACAGAAGAAAGG
UPH 3 ' KO genotyping	GACCTGCAGCCCAAGCTA	CCCTTGCAAACAGAAGAAAGG
tdTO 5 ' WT genotyping	CTCCTCTCCGGACAAGAATC	TGCTGCAAATGAGTGTGG
tdTO 5 ' KO genotyping	CTCCTCTCCGGACAAGAATC	ATGACCTCCTCGCCCTTG
tdTO 3 ' WT genotyping	AGAGAACGCGGATGAGACCT	CCCTTGCAAACAGAAGAAAGG
tdTO 3 ' KO genotyping	GACCTGCAGCCCAAGCTA	CCCTTGCAAACAGAAGAAAGG
Southern BamHI probe	TGGTTTTCTTGTCGTTGCTG	CTGACTGGGTCCTTGAGCAT
Southern NdeI probe	TCCTGGGAAGGCACTATGTC	ACCTTCTCCTGCCCTTCATT
Hand1 ISH probe	CCATCATCACCACTCACACC	GCGCCCTTTAATCCTCTTCT
Nkx2-5 ISH probe	TATGGCTACAACGCCTACCC	GTGTGGAATCCGTCGAAAGT
ASO negative control	AACACGTCTATACGC	
ASO UPH A	GCTAGTTAAGCAGGA	
ASO UPH B	ATTCAATTTAGGTCAT	
5GSP1		CAGCTGTATGGGCTCAGGTGACTGC
3GSP1		TGGAGATGGGCTACCATTGGTGTTGA
AP1	CCATCCTAATACGACTCACTATAGGGC	
Hand2 - Gata site	TTTACCCACTGGTCCCCTCT	TGGACAACATGGGACAGAAA
Nkx2-5 - Gata site	CTGCAACTATCACCCGGAAT	AGAAACCCCCATCTGTTTCC
UPH ChIP site 1	TCACCTCCCCATGTCTTTTC	GAGGAACCTGCATTGCTTTC
UPH ChIP site 2	ACCTCGGGCTTTCGATCTTA	GCTTGGGAAGGTAAGCCTTT

SEQUENCE NAME	FORWARD	REVERSE
UPH ChIP site 3	GAAACTAGCCTTGCCCCTTC	GGGTGCCTAGGGAGGAATAC
Nkx2-5 ChIP - site 1	ACTGTGAAGCCCAATTCCAG	AACCAGAAATTGTGGCAAGG

Supplementary Material

Refer to Web version on PubMed Central for supplementary material.

Acknowledgments

We thank D. Tennison for technical assistance and J. Cabrera for graphics. We thank the Histopathology Core Facility at University of Texas Southwestern for histology. This work was supported by grants from the National Institutes of Health (HL-077439, AR-067294, HL-130253, DK-099653 and U01-HL-100401), Fondation Leducq Networks of Excellence, Cancer Prevention and Research Institute of Texas and the Robert A. Welch Foundation (grant 1-0025 to E.N.O.), a pre-doctoral fellowship from the American Heart Association (14PRE19830031) to K.M.A. and a Muscular Dystrophy Association Development Grant (MDA377340) to D.M.A.

References

1. Srivastava D, et al. Regulation of cardiac mesodermal and neural crest development by the bHLH transcription factor, dHAND. Nat. Genet. 1997; 16:154–160. [PubMed: 9171826]
2. Han Z, Yi P, Li X, Olson EN. Hand, an evolutionarily conserved bHLH transcription factor required for *Drosophila* cardiogenesis and hematopoiesis. Development. 2006; 133:1175–1182. [PubMed: 16467358]
3. Song K, et al. Heart repair by reprogramming non-myocytes with cardiac transcription factors. Nature. 2012; 485:599–604. [PubMed: 22660318]
4. Conway SJ, Firulli B, Firulli AB. A bHLH code for cardiac morphogenesis. Pediatr. Cardiol. 2010; 31:318–324. [PubMed: 20033146]
5. Yamagishi H, Olson EN, Srivastava D. The basic helix-loop-helix transcription factor, dHAND, is required for vascular development. J. Clin. Invest. 2000; 105:261–270. [PubMed: 10675351]
6. Charité J, et al. Role of Dlx6 in regulation of an endothelin-1-dependent, dHAND branchial arch enhancer. Genes Dev. 2001; 15:3039–3049. [PubMed: 11711438]
7. McFadden DG, et al. A GATA-dependent right ventricular enhancer controls dHAND transcription in the developing heart. Development. 2000; 127:5331–5341. [PubMed: 11076755]
8. Hnisz D, et al. Super-enhancers in the control of cell identity and disease. Cell. 2013; 155:934–947. [PubMed: 24119843]
9. Lepoivre C, et al. Divergent transcription is associated with promoters of transcriptional regulators. BMC Genomics. 2013; 14:914. [PubMed: 24365181]
10. Voth H, et al. Co-regulated expression of HAND2 and DEIN by a bidirectional promoter with asymmetrical activity in neuroblastoma. BMC Mol. Biol. 2009; 10:28. [PubMed: 19348682]
11. Chodroff RA, et al. Long noncoding RNA genes: conservation of sequence and brain expression among diverse amniotes. Genome Biol. 2010; 11:R72. [PubMed: 20624288]
12. Kambara H, et al. Regulation of interferon-stimulated gene BST2 by a lncRNA transcribed from a shared bidirectional promoter. Front. Immunol. 2015; 5:676. [PubMed: 25688240]
13. Uesaka M, et al. Bidirectional promoters are the major source of gene activation-associated non-coding RNAs in mammals. BMC Genomics. 2014; 15:35. [PubMed: 24438357]
14. Anderson DM, et al. A micropeptide encoded by a putative long noncoding RNA regulates muscle performance. Cell. 2015; 160:595–606. [PubMed: 25640239]
15. Nelson BR, et al. A peptide encoded by a transcript annotated as long noncoding RNA enhances SERCA activity in muscle. Science. 2016; 351:271–275. [PubMed: 26816378]
16. Grote P, et al. The tissue-specific lncRNA *Fendrr* is an essential regulator of heart and body wall development in the mouse. Dev. Cell. 2013; 24:206–214. [PubMed: 23369715]
17. Wang KC, et al. A long noncoding RNA maintains active chromatin to coordinate homeotic gene expression. Nature. 2011; 472:120–124. [PubMed: 21423168]
18. Yang YW, et al. Essential role of lncRNA binding for WDR5 maintenance of active chromatin and embryonic stem cell pluripotency. eLife. 2014; 3:e02046. [PubMed: 24521543]
19. Stein CA, et al. Efficient gene silencing by delivery of locked nucleic acid antisense oligonucleotides, unassisted by transfection reagents. Nucleic Acids Res. 2010; 38:e3. [PubMed: 19854938]
20. Kaikkonen MU, et al. Remodeling of the enhancer landscape during macrophage activation is coupled to enhancer transcription. Mol. Cell. 2013; 51:310–325. [PubMed: 23932714]

21. Kim TK, et al. Widespread transcription at neuronal activity-regulated enhancers. Nature. 2010; 465:182–187. [PubMed: 20393465]
22. Schmitt S, Prestel M, Paro R. Intergenic transcription through a polycomb group response element counteracts silencing. Genes Dev. 2005; 19:697–708. [PubMed: 15741315]
23. Herzog VA, et al. A strand-specific switch in noncoding transcription switches the function of a Polycomb/Trithorax response element. Nat. Genet. 2014; 46:973–981. [PubMed: 25108384]
24. Ho Y, Elefant F, Liebhaber SA, Cooke NE. Locus control region transcription plays an active role in long-range gene activation. Mol. Cell. 2006; 23:365–375. [PubMed: 16885026]
25. He A, et al. Dynamic GATA4 enhancers shape the chromatin landscape central to heart development and disease. Nat. Commun. 2014; 5:4907. [PubMed: 25249388]
26. Jonkers I, Lis JT. Getting up to speed with transcription elongation by RNA polymerase II. Nat. Rev. Mol. Cell Biol. 2015; 16:167–177. [PubMed: 25693130]
27. Yanagisawa H, Clouthier DE, Richardson JA, Charité J, Olson EN. Targeted deletion of a branchial arch-specific enhancer reveals a role of dHAND in craniofacial development. Development. 2003; 130:1069–1078. [PubMed: 12571099]
28. Barron F, et al. Downregulation of Dlx5 and Dlx6 expression by Hand2 is essential for initiation of tongue morphogenesis. Development. 2011; 138:2249–2259. [PubMed: 21558373]
29. Charité J, McFadden DG, Olson EN. The bHLH transcription factor dHAND controls Sonic hedgehog expression and establishment of the zone of polarizing activity during limb development. Development. 2000; 127:2461–2470. [PubMed: 10804186]
30. Lucas ME, Müller F, Rüdiger R, Henion PD, Rohrer H. The bHLH transcription factor *hand2* is essential for noradrenergic differentiation of sympathetic neurons. Development. 2006; 133:4015–4024. [PubMed: 17008447]
31. Anderson DM, et al. Mohawk is a novel homeobox gene expressed in the developing mouse embryo. Dev. Dyn. 2006; 235:792–801. [PubMed: 16408284]
32. Shelton JM, Lee MH, Richardson JA, Patel SB. Microsomal triglyceride transfer protein expression during mouse development. J. Lipid Res. 2000; 41:532–537. [PubMed: 10744773]
33. Gagnon KT, Li L, Janowski BA, Corey DR. Analysis of nuclear RNA interference in human cells by subcellular fractionation and Argonaute loading. Nat. Protocols. 2014; 9:2045–2060. [PubMed: 25079428]
34. Conrad NK. Chapter 15. Co-immunoprecipitation techniques for assessing RNA-protein interactions in vivo. Methods Enzymol. 2008; 449:317–342. [PubMed: 19215765]
35. ENCODE Project Consortium. An integrated encyclopedia of DNA elements in the human genome. Nature. 2012; 489:57–74. [PubMed: 22955616]

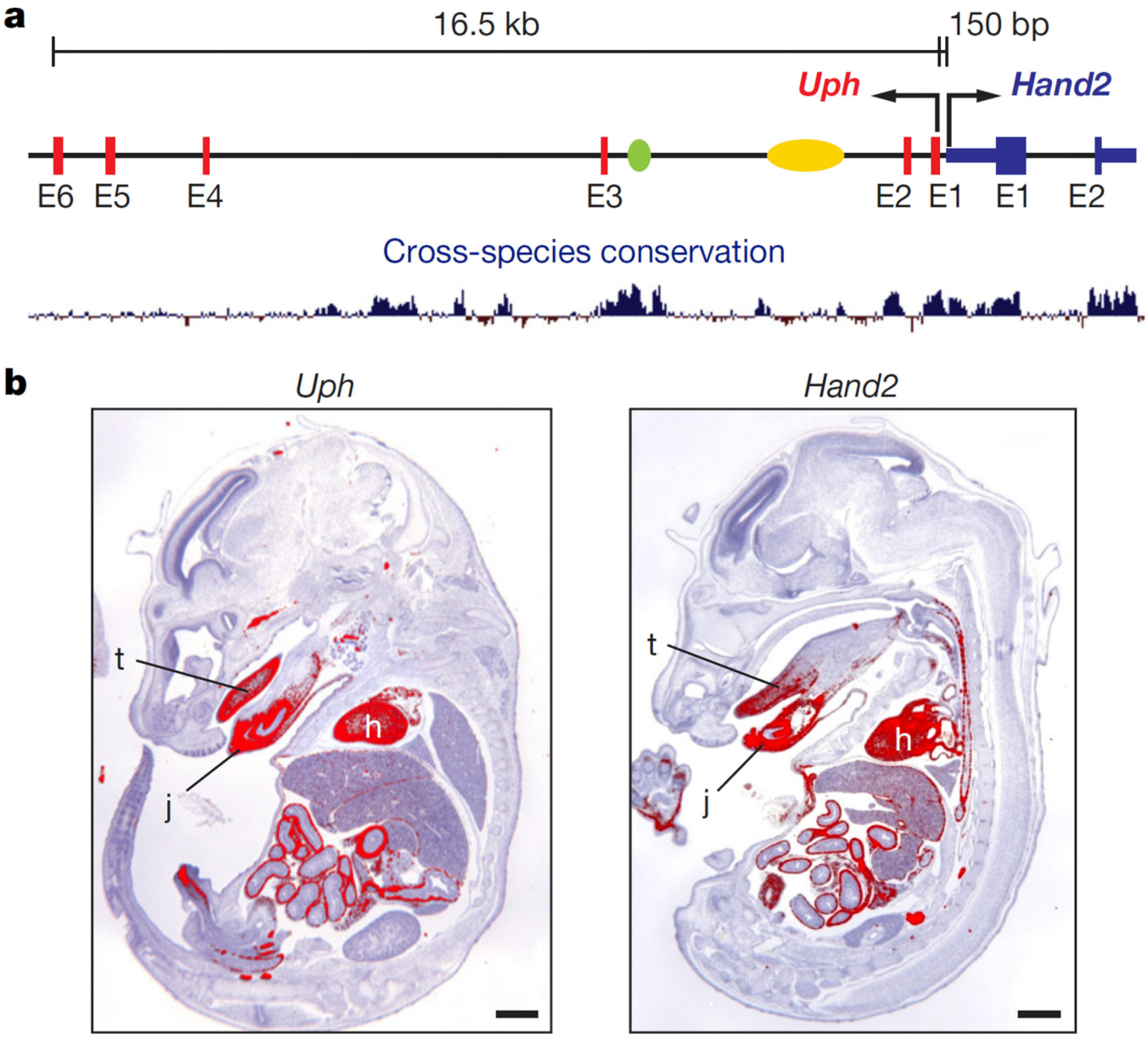

Figure 1. Co-expression of upperhand (*Uph*) and *Hand2*

a, The mouse *Uph–Hand2* locus. *Uph* is transcribed 150 bp upstream of *Hand2* and contains two *Hand2* enhancers (branchial arch enhancer (green) and cardiac enhancer (yellow)) within one of its introns. Bottom, mammalian sequence conservation (blue). **b**, Section *in situ* hybridization of E15.5 mouse embryos for either *Uph* (left) or *Hand2* (right). Expression was detected in heart (h), tongue (t) and jaw (j). Scale bars, 1 mm.

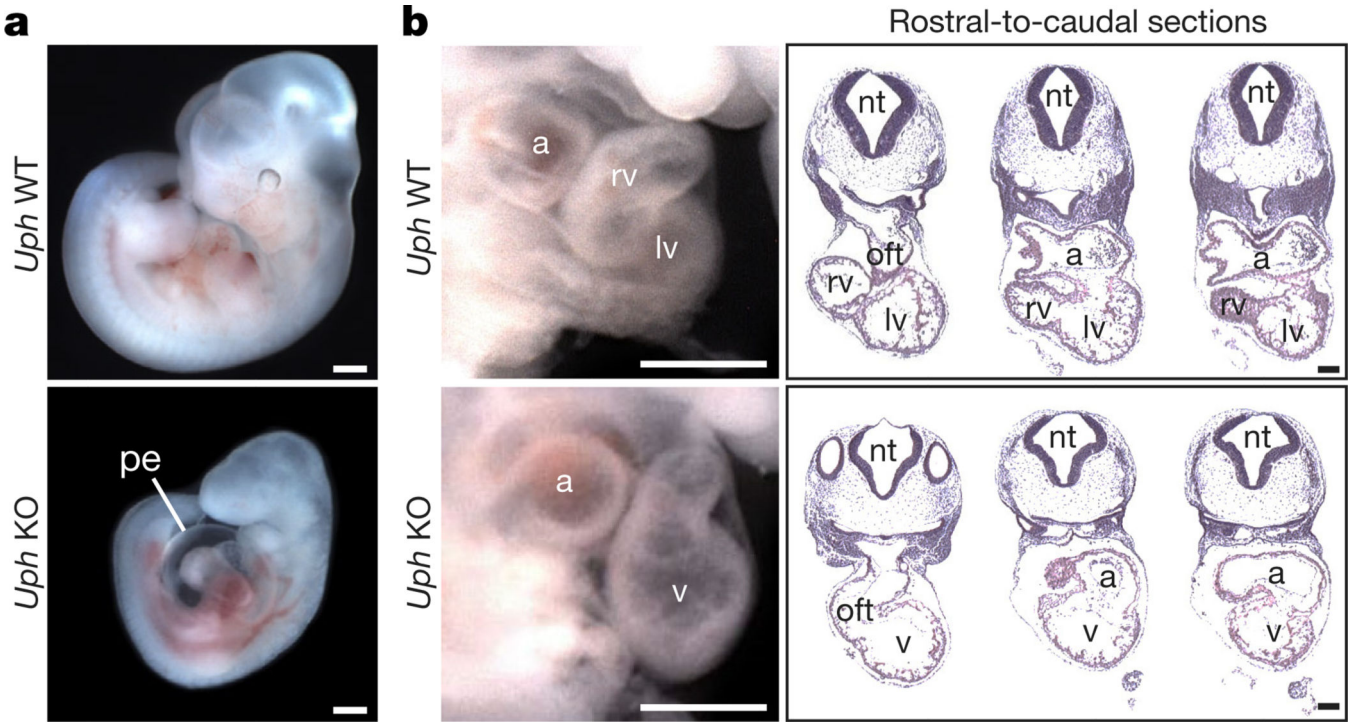

Figure 2. Cardiac defects of *Uph* KO embryos

a, At E10.5, *Uph* KO embryos have pericardial effusion (pe) and appear smaller than wildtype (WT) littermate embryos. **b**, At E10.5, wild-type embryos (top) have distinct right and left ventricular (rv and lv, respectively) chambers, whereas *Uph* KO embryos (bottom) have a single ventricle (v). This abnormality is highlighted in rostral-to-caudal sections through the heart (left to right). a, atria; nt, neural tube; oft, outflow tract. Scale bars, 500 μm (**a**) and 100 μm (**b**).

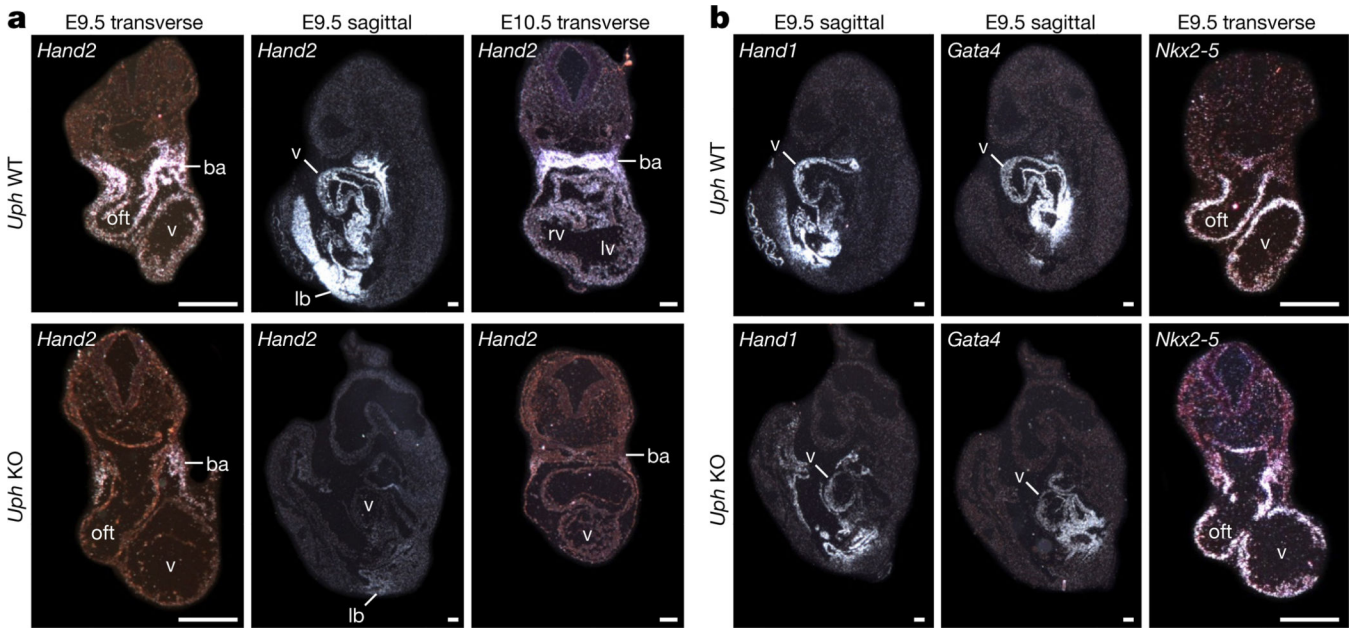

Figure 3. Loss of cardiac *Hand2* expression in *Uph* KO embryos

a, *In situ* hybridizations of wild-type and *Uph* KO embryos at E9.5 (transverse and sagittal sections) and E10.5 (transverse) show loss of *Hand2* expression in the heart of *Uph* KO embryos, with detectable expression in the branchial arches (ba) and limb bud (lb). **b**, *In situ* hybridizations of wild-type and *Uph* KO embryos at E9.5 (transverse and sagittal sections) using *Hand1*, *Gata4* or *Nkx2-5* probes. Scale bars, 100 μ.

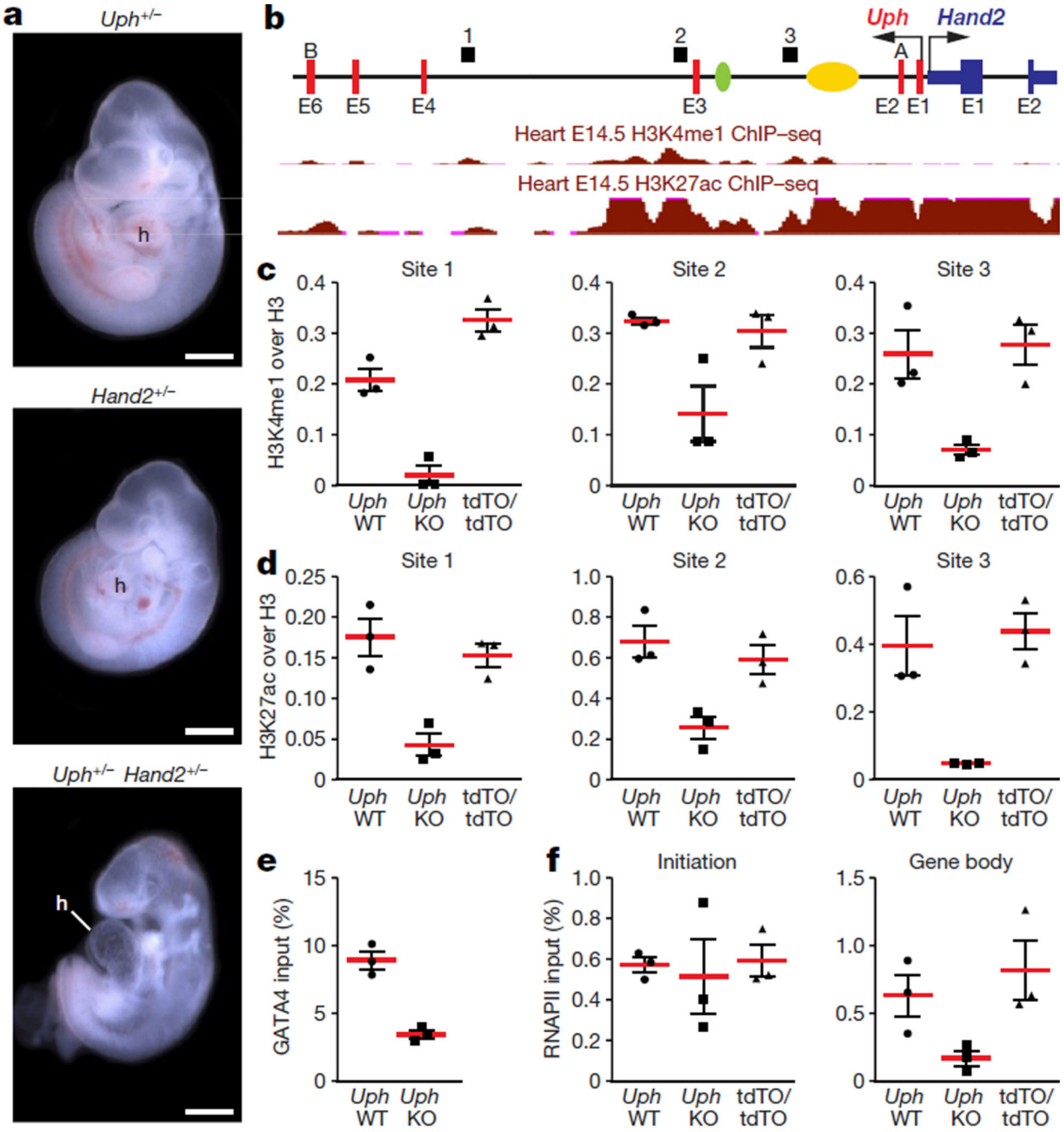

Figure 4. *Uph* transcription in *cis* is required for active enhancer marks in the *Uph* locus and RNAPII elongation at the *Hand2* gene

a, E10.5 embryos heterozygous for either *Uph* (top) or *Hand2* (middle) appear normal in size and morphology. By contrast, $Uph^{+/-}$ $Hand2^{+/-}$ double heterozygote embryos developed a single ventricle. Scale bars, 1 mm. **b**, *Uph–Hand2* locus with letters (A or B) indicating GapmeR target sites, and numbers (1–3) indicating the regions analysed by qPCR following ChIP. The *Hand2* branchial arch enhancer (green) and cardiac enhancer (yellow) are indicated. Shown in red are the ENCODE/LICR ChIP followed be sequencing (ChIP–seq) tracks for H3K4me1 and H3K27ac active enhancer markers. E1–E6, exons 1–6. See

Methods for source data. **c, d**, H3K4me1 (**c**) and H3K27ac (**d**) modifications present at the *Uph* locus in E10.0 wild-type hearts are reduced in *Uph* KO hearts, and unchanged in $Uph^{tdTO/tdTO}$ homozygous hearts. Values are normalized to total histone H3. **e**, GATA4 binding to the cardiac enhancer is reduced in E10.0 knockout hearts relative to wild type. **f**, ChIP using RNAPII (phosphoS2) antibody at the *Hand2* transcriptional start site or gene body in wild-type, *Uph* KO and $Uph^{tdTO/tdTO}$ homozygous hearts. Values normalized as a percentage of total input chromatin. Each point is one of three technical replicates of five pooled hearts for each genotype in each ChIP experiment, from one of two independent experiments; data are mean ± s.e.m.